

# Topological kicks enhance colloidal diffusivity in topological turbulence

Timofey Kozhukhov,<sup>1,2</sup> Benjamin Loewe,<sup>3</sup> Kristian Thijssen,<sup>2</sup> and Tyler N. Shendruk<sup>1</sup>

<sup>1</sup>*School of Physics and Astronomy, University of Edinburgh, Peter Guthrie Tait Road, Edinburgh, EH9 3FD, UK.*

<sup>2</sup>*Niels Bohr Institute, University of Copenhagen, Blegdamsvej 17, Copenhagen, Denmark.*

<sup>3</sup>*Facultad de Física, Pontificia Universidad Católica de Chile, Santiago 7820436, Chile.*

(Dated: March 26, 2025)

Colloidal inclusions in nematic fluids induce topological defects that govern their dynamics. These defects create well-understood rheological behavior in passive nematics, but the interplay between colloid-associated defects and spontaneously generated activity-induced defects introduces new dynamical regimes in active nematic turbulence. Using mesoscale simulations, we study the motion of colloids with strong anchoring in an active nematic and find effective colloid diffusivity exhibits a striking non-monotonic dependence on activity. At low activities, *topological kicks* from the motile activity-induced bulk defects drive frequent rearrangements of the colloid-associated defects, enhancing colloidal transport. At high activity, defect interactions become isotropic, decorrelating colloidal motion and reducing the effective diffusivity. Our results reveal how the competition between colloid-associated and activity-induced defects fundamentally shapes transport in active nematics.

Many intrinsically out-of-equilibrium biological materials have recently been shown to exhibit nematic symmetry [1]. Examples include subcellular filaments [2–4], bacterial biofilms [5, 6] and cell monolayers [7–10]. These typically do not exhibit global symmetry breaking, but rather include local disruptions to the orientational order, known as topological defects, which are increasingly recognized as key to determining biomaterial properties [10–15], just as they are in passive materials [16]. Defects act as biological hotspots, influencing apoptosis [17], neural mound formation [18], and limb development in Hydra [4]. For this reason, they offer a pathway toward designing life-like synthetic materials [11, 12].

Defects can be induced in passive liquid crystals by strong anchoring to boundaries, as occurs when colloids are suspended in nematics [19]. In three dimensions, they form entangled disclination lines [20], while they form tightly bound colloid-defect pair complexes [19]. Defects interact dynamically with their environments, yielding intriguing properties, such as disclination knotting in nematic gels [21], lock-key control [22], optical trapping [11] and tunable three-dimensional architecture [23].

Another strategy for creating defects is through energy injection, via temperature gradients, shearing or local biological activity. In active nematics, local energy input is converted into mechanical work, continuously driving defect nucleation [24], which maintains a non-zero steady-state defect density [25, 26]. Active nematic defects exhibit unique non-equilibrium properties, such as self-propulsion [27], which can profoundly influence collective dynamics [28] and lead to active—or topological—turbulence [29].

Despite extensive studies of both active nematics and colloidal systems, the interplay between colloid-induced surface defects and bulk defects in active fluids remains uninvestigated. Studies of geometry-induced dynamics, such as active nematics on the surface of a toroid [30], confined to boundaries [31] or within emulsions [32, 33], have revealed rich and complex behaviors. Similarly,

early studies on colloidal solutes in active solvents have shown activity alters effective transport dynamics [34–37] and interactions with boundaries [38]. However, few studies have explored systems in which active stresses sustain a steady-state population of defects that interact with colloid-induced surface defects. This represents an unexplored avenue for potentially anomalous behaviors.

In this manuscript, we investigate how the active topological environment surrounding strongly anchored normal homeotropic colloids influences the dynamics in active nematic topological turbulence. We uncover striking results for the effective diffusivity of colloids, revealing a non-monotonic dependence on dimensionless activity, which arises due to interactions between colloid-associated companion defects and activity-induced bulk defects.

The coarse-grained mesoscale simulation technique Multi-Particle Collision Dynamics (MPCD; § SI) is used to model the orientational fluid in the limit of a one-viscosity and one-elastic constant approximation,  $K$  [39]. This approach has been employed to simulate polymer-nematic mixtures [40] and colloidal liquid crystals [20]. A strongly anchored colloid in a passive nematic induces a pair of nearby  $-1/2$  defects (Fig. 1a.i). We refer to the colloid-associated defects as *companion defects* and the structure as a *colloid-companion complex*. In a passive nematic, the colloid-companion complex has a neutral topological charge. The nematic MPCD fluid is given *extensile* activity by including a local active stress  $\alpha \geq 0$ , resulting in an active length scale  $\ell_\alpha \sim (K/\alpha)^{1/2}$  corresponding to the average spacing between nematic defects [41]. The active length scale can be compared to colloid radius through the dimensionless activity number

$$A = \left(\frac{R_C}{\ell_\alpha}\right)^2 \left(1 + 2\frac{R_C}{\ell_\alpha}\right)^{-1}. \quad (1)$$

Specifically,  $A$  compares the colloidal area  $\pi R_C^2$  to the area of an annulus of width  $\ell_\alpha$  around the colloid

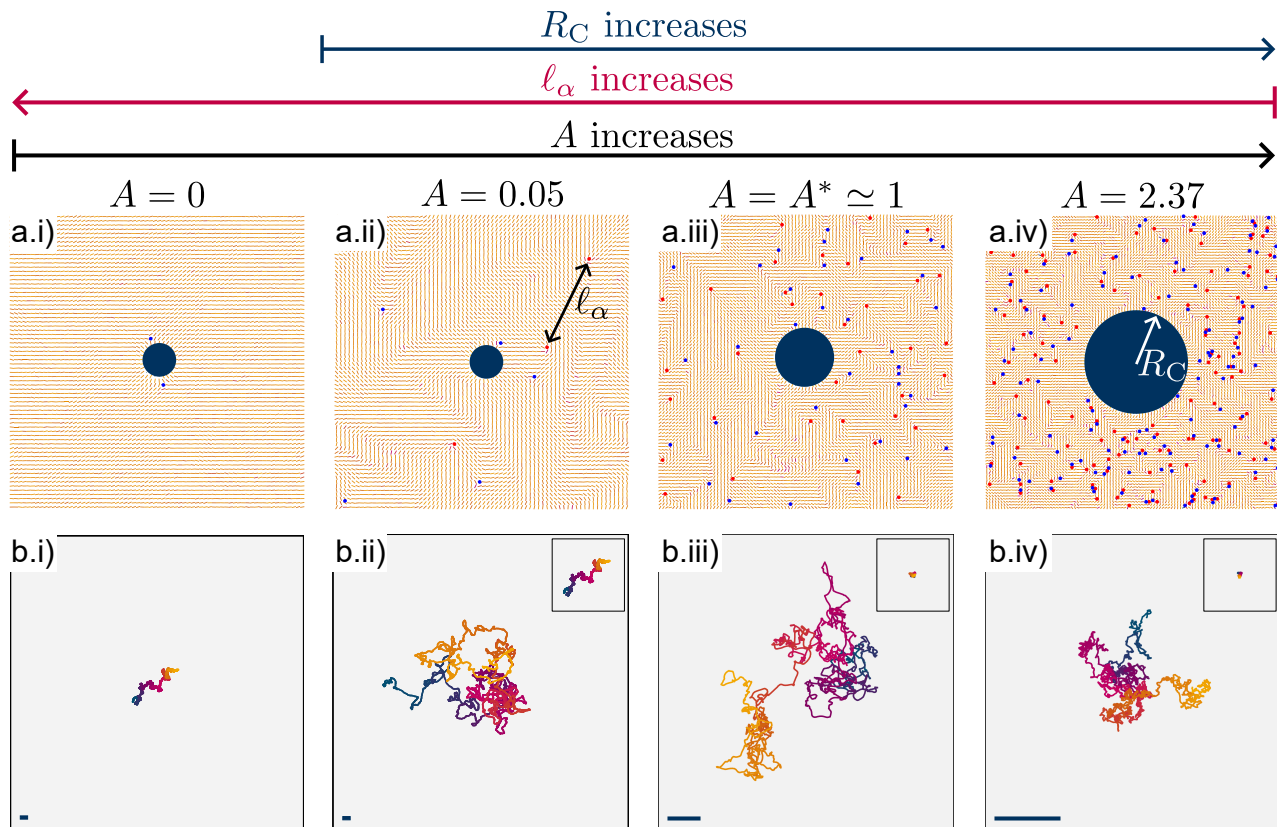


FIG. 1. **Topological turbulence enhances displacement of strongly anchored colloids.** (a) Director field snapshots for varying activity number,  $A$ . Red and blue dots denote  $+1/2$  and  $-1/2$  defects, respectively. *i.*  $A = 0$  *ii.*  $0.27$  *iii.*  $0.67$  *iv.*  $2.37$  (b) Colloid trajectories over  $3 \times 10^5$  timesteps. Each trajectory colored by time and each domain covers the same area of  $\ell_{\text{sys}}^2 = 160^2$ , with scale bars indicating the colloid radius. Insets show a passive trajectory of a colloid with identical radius.

$\pi(\ell_\alpha^2 + 2R_C\ell_\alpha)$ . When  $A > 1$ , the colloid is large compared to the intrinsic length scale of the topological turbulence, whereas the colloid is small compared to the distance between activity-induced defects when  $A < 1$ .

When activity is sufficient to produce topological turbulence, the active stress induces the continuous nucleation of defects in bulk away from the colloid. For low activity, one of the two companion defects is frequently lost from the colloid-companion complex — only a single  $-1/2$  companion defect remains bound to the colloid (Fig. 1a.ii, Movie M1). This structure persists to intermediate activities (Fig. 1a.iii, Movie M2), but, at higher activities, a sea of topological defects surrounds the colloid, such that the notion of well-defined companion defects becomes ill-defined (Fig. 1a.iv, Movie M3). This change in topological configuration will be shown to have profound effects on the dynamics (Fig. 1b).

Example trajectories illustrate that the displacement of the colloid-companion complex increases as activity increases (Fig. 1b.i-ii) to a maximum (Fig. 1b.iii) but reduces once the colloid loses both companion defects (Fig. 1b.iv). In all cases, the active systems exhibit enhanced diffusivity compared to an identically sized colloid in a passive nematic (Fig. 1b insets). This difference

is quantified by the mean-squared displacement (MSD, § II; Fig. S1) of the colloid trajectories. The instantaneous speed  $v_0$  of the colloid obtained from the MSD increases with activity  $A$  (Fig. 2a) and plateaus as activity increases above a value of  $A^* \simeq 0.67$ . Simultaneously, the decorrelation time  $\tau_r$  of the colloid monotonically decreases with  $A$  (Fig. 2b). These changes in relaxation time and speed result in a peak in the effective diffusivity  $D$  relative to its thermal counterpart  $D_0$  (Fig. S2) around a critical activity  $A^* = 0.67$  (Fig. 2c). This reveals that not only does the active component of diffusivity  $v_0^2\tau_r$  dominate over the passive thermal component, but is maximized when the colloidal size equals the active length scale, *i.e.*  $A = A^* \simeq 1$ . The dynamics uncovered here of the strongly anchored colloid are unlike the behaviors of unanchored colloids, which lack companion defects. While unanchored colloids exhibit monotonically increasing speed (Fig. 2a), their decorrelation time remains small and nearly constant (Fig. 2b; § SIII). The unanchored colloids exhibit enhanced diffusivity, as is to be expected since the active flows increase dispersion, but do not exhibit a maximum, indicating that the maximum in effective diffusivity is due to the interplay between companion defects and the topological

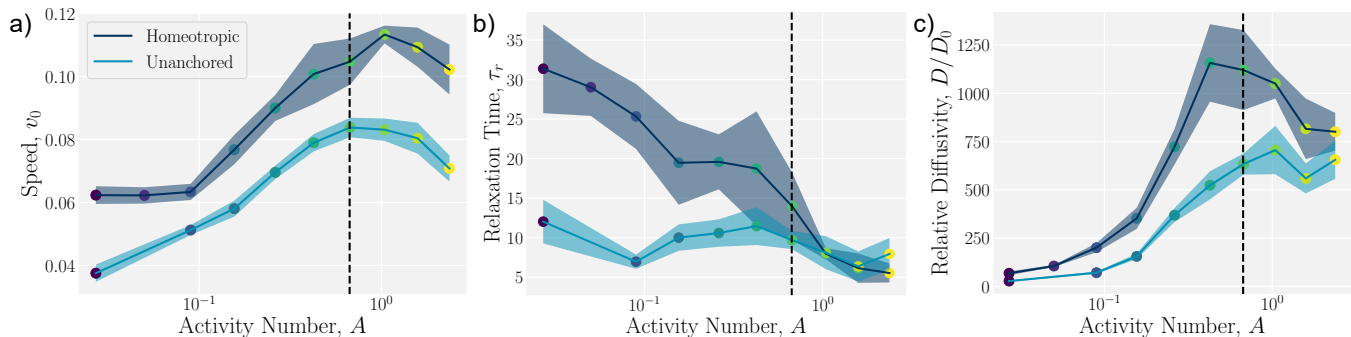


FIG. 2. **Mean-squared displacement (MSD) dynamics of passive colloids in topological turbulence.** Measured fit values from MSDs. Shaded regions represents the standard deviation between realizations, and the dashed line represents  $A = A^*$ . **(a)** Speed  $v_0$ . **(b)** Decorrelation time  $\tau_r$ . **(c)** Relative diffusivity  $D/D_0$ . Strongly anchored homeotropic colloids exhibit non-monotonicity, whereas unanchored colloids do not.

turbulence.

The colloidal dynamics are due to changes to the colloid-companion complex structure. For low activities, the  $-1/2$  defect distribution is highly localized around the colloid, with increases to the activity homogenizing this distribution (Fig. S3a; § SIV). However, the average distance of the closest  $-1/2$  defect to the colloid decreases with activity (Fig. S3b-c), which allows the definition of a *near-colloid region* within which the number of  $-1/2$  defects  $N_C$  can be counted (Fig. 3a). At low activity,  $N_C \approx 1$  with a high probability of finding a single defect (Fig. S4). At higher activities,  $N_C$  rises steadily, and the structure of the surrounding defects becomes more gas-like.

The observation of a single companion defect at low activities is at odds with the expectation from passive nematics [19], suggesting the loss of one companion  $-1/2$  defect is facilitated by the topological turbulence. Self-propelled  $+1/2$  defects in the surrounding turbulence are continuously created and annihilated, with annihilation events occurring because of the attraction between oppositely charged defects [42, 43]. Indeed, as an activity-induced  $+1/2$  defect from the bulk turbulence approaches the colloid-companion complex, it modifies the elastic energy landscape. A simplified model of the elastic interactions between a colloid-companion complex with a colloid of  $+1$  charge, two antipodal  $-1/2$  companion defects and an approaching activity-induced  $+1/2$  defect from the surrounding steady-state population of defects (§ SV; Fig. S5a) shows that the energy barrier for the bound companion defect is large when the  $+1/2$  defect is far from the complex (Fig. S5b). However, when the  $+1/2$  defect is sufficiently close, the potential barrier of the nearest  $-1/2$  shrinks to zero, allowing it to escape into the bulk turbulence. Moreover, the loss of one companion defect enhances the elastic binding between the remaining companion defect and the colloid (§ SV; Fig. S5c). Thus, the remaining colloid-companion complex with only a single bound defect is more stable and maintains a non-neutral charge of  $+1/2$ , which further repels  $+1/2$  defects.

Since the colloid-companion complex with a single bound  $-1/2$  defect has a net  $+1/2$  charge, it possesses orientational symmetry breaking (Fig. 3a inset). In the colloidal reference frame (Fig. 3b, Fig. S6),  $-1/2$  defects are not uniformly distributed around the colloid at low activities (Fig. 3b.i). Instead, defects have a higher probability of being found trailing the colloid's direction of motion. This anisotropy persists as the activity approaches  $A^*$  (Fig. 3b.ii), but the distribution becomes radially symmetric at the highest activities (Fig. 3b.iii), as quantified by distributions of relative angles (§ SVI; Fig. S7).

Since the structure of the single-companion complex in the far-field limit (is equivalent to a  $+1/2$  defect (Fig. 3a inset), one might suppose that the net  $+1/2$  topological charge of the colloid-companion complex endows it with the self-motility of an effective  $+1/2$  defect, which would cause it to move away from the primary played region towards the primarily bend region in front in extensible active fluids [44]. Surprisingly, this effective  $+1/2$  far-field director pattern would imply motion in the opposite direction to the observed colloidal motion. Thus, the enhanced diffusion is not directly due to the effective  $+1/2$  topological structure of the colloid-companion complex, but due to a secondary effect.

The colloid-companion complex moves in the opposite direction due to the interplay between the colloid-companion complex and activity-induced  $+1/2$  defects from the surrounding topological turbulence (Fig. 4a). The incoming  $+1/2$  defects are predominantly found in the direction opposite to the direction of the colloid velocity at low activities (§ SVII; Fig. 4a.i). This is because they are attracted to the remaining  $-1/2$  companion defect. As an activity-induced  $+1/2$  defect approaches the companion, it experiences an elastic attraction to the companion  $-1/2$  defect, while also producing an active flow (Fig. 4a.ii) [27]. The flows generated by the approaching  $+1/2$  defect advect the colloid, pushing it away from the approaching  $+1/2$  and companion  $-1/2$  defects (Fig. 4a.iii). However, rather than annihilate with the companion, the  $+1/2$  defect performs a *topological kick*

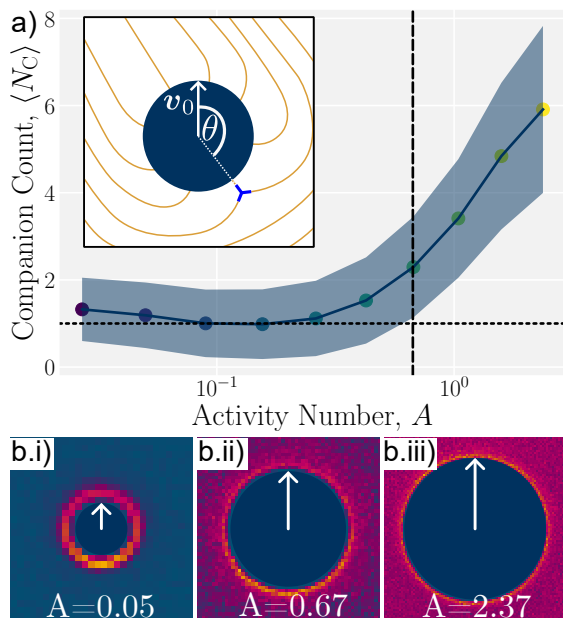


FIG. 3. **Radial symmetry breaking of  $-1/2$  defects.** (a) Average number of  $-1/2$  defects  $N_C$  in the near colloid region. Shaded region represents standard deviation between realizations, dashed line represents  $A = A^*$  and dotted line represents a single companion defect bound to the colloid. (inset) Schematic of defect angle  $\theta$  with respect to colloid velocity  $v_0$ . Complexes with a single companion form a far-field equivalent a  $+1/2$  defect, oriented towards the companion. (b) Distribution of  $-1/2$  defects in the moving colloid reference frame (white arrow). Blue represents low probability and yellow high. Distributions for all considered activity numbers are shown in Fig. S6.

to the colloid as it is deflected (Fig. 4a.iv).

The effective energy landscape experienced by the  $+1/2$  defect as it approaches the complex explains its deflection, rather than annihilation (§ SVIII). The effective potential is obtained by considering the elastic energy with the colloid-companion complex and a linear potential that models a constant active self-propulsive force. Crucially, the colloidal monopole and the dipole center are off-set, with the dipole laying closer to the  $+1/2$  defect. The resulting effective potential due to elastic interactions, anchoring, and self-motility is saddle-like in nature (Fig. 4b; Eq. S9), which is illustrated by a typical Langevin trajectory taken by an activity-induced  $+1/2$  defect as it approaches the complex (Fig. 4b).

It is by this very mechanism that the colloid-companion complex is kicked through the topological turbulence with enhanced diffusion:  $+1/2$  defects are attracted to the companion defect of the colloid, seeking to annihilate, but are instead deflected by the elastic forces from colloidal anchoring. The flow fields produced by the self-motile  $+1/2$  defect push the colloid-companion complex away, in the direction opposite the  $-1/2$  companion defect, resulting in enhanced colloidal diffusivity. This is the opposite direction as would be expected due

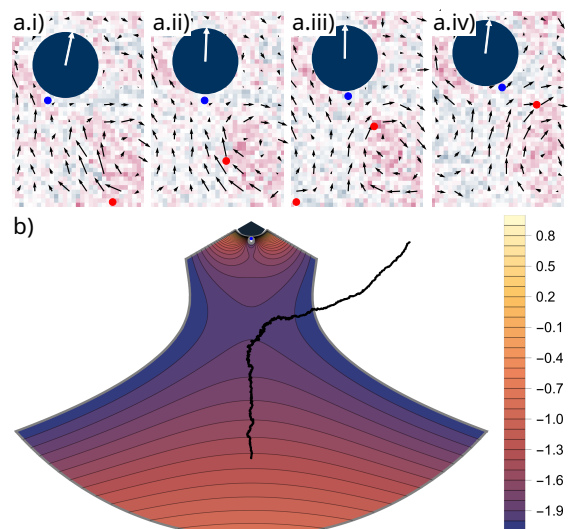


FIG. 4. **Attempted annihilation of a  $-1/2$  companion defect by an activity-induced  $+1/2$  defect results in enhanced colloidal diffusivity.** (a) Simulation snapshots of velocity (black arrows) and vorticity (color map) at the critical activity  $A^* \simeq 0.67$ . Snapshots are cropped and rotated from a fixed space within the simulation domain, visible in Movie M4. The white arrow indicates instantaneous colloid direction of motion and defects marked as in Fig. 1. a.i) Time  $t = 1680\delta t$ ; a.ii)  $1780\delta t$ ; a.iii)  $1880\delta t$ ; a.iv)  $2010\delta t$ ; (b) The potential  $U_{\text{eff}}$  experienced by a  $+1/2$  defect approaching a colloid-defect complex (Eq. S9). Example Langevin trajectory of a  $+1/2$  defect plotted as a black line, illustrating typical deflection dynamics.

to the effective  $+1/2$  topological charge of the colloid-companion complex (Fig. 3a inset). At low activity numbers, the lower number of  $+1/2$  defects in the fluid bulk causes fewer of these events to occur. Thus, the colloid-companion complex is slower (Fig. 2a) but the persistence time is longer  $\tau_r$  (Fig. 2b). As the activity number increases, the number of  $+1/2$  defects in the fluid bulk increases, leading to more near-annihilation events, with an increase in the instantaneous colloidal motion but decrease in persistence time and a loss of anisotropy. In this way, the model also explains the non-monotonic diffusivity observed in strongly anchored homeotropic colloids, but not in unanchored colloids.

There is a rich history of research investigating the dynamics of colloidal particles in passive nematics, showing how topological interactions arising through anchoring can lead to the formation of defect structures [20] and colloidal self-assembly [45, 46]. Activity restructures the topological environment of the colloid from a neutral colloid-companion complex to a positively charged colloid-companion complex to a particle in a gas of activity-induced defects. Our results begin to extend this understanding to active nematics, where spontaneous flows and self-propelled defects have already been shown to rectified motion in chiral inclusions [37, 47], enhance mixing properties of tracers above active carpets [48], and

generate complex motion in emulsions [33]. The introduction of anchoring in active nematics, as explored here, reveals a novel mechanism by which the colloid-defect interactions are fundamentally altered, leading to enhanced colloidal diffusivity and defect-mediated propulsion arising from topological kicks.

This study focused on strong normal anchoring at the surface, but planar anchoring is also common in the passive nematic colloidal literature. The resulting colloid also has an effective +1 topological charge [19], and may similarly lead to enhanced diffusivity. While this work has primarily focused on how active nematics influence colloidal dynamics, it also reveals how colloidal inclusions—through anchoring and defect interactions—reciprocally influence the structure and flow of the active nematic medium. This dual interaction opens the door to using colloids as a means of manipulating and control-

ling defect behavior in active systems, ultimately paving the way for the exploration of colloidal self-assembly in topological turbulence as an emergent and tunable phenomenon.

*Acknowledgments* We acknowledge useful discussions with Davide Marenduzzo. This research has received funding from the European Research Council (ERC) under the European Union’s Horizon 2020 research and innovation programme (Grant agreement No. 851196). This work was further supported by the Novo Nordisk Foundation grants no. NNF18SA0035142 and NNF23OC0085012. For the purpose of open access, the author has applied a Creative Commons Attribution (CC BY) license to any Author Accepted Manuscript version arising from this submission.

- 
- [1] M. C. Marchetti, J.-F. Joanny, S. Ramaswamy, T. B. Liverpool, J. Prost, M. Rao, and R. A. Simha, *Hydrodynamics of soft active matter*, *Reviews of Modern Physics* **85**, 1143 (2013).
- [2] T. Sanchez, D. T. Chen, S. J. DeCamp, M. Heymann, and Z. Dogic, *Spontaneous motion in hierarchically assembled active matter*, *Nature* **491**, 431 (2012).
- [3] R. Zhang, N. Kumar, J. L. Ross, M. L. Gardel, and J. J. De Pablo, *Interplay of structure, elasticity, and dynamics in actin-based nematic materials*, *Proceedings of the National Academy of Sciences* **115**, E124 (2018).
- [4] Y. Maroudas-Sacks, L. Garion, L. Shani-Zerbib, A. Livshits, E. Braun, and K. Keren, *Topological defects in the nematic order of actin fibres as organization centres of hydra morphogenesis*, *Nature Physics* **17**, 251 (2021).
- [5] D. Dell’Arciprete, M. L. Blow, A. T. Brown, F. D. Farrell, J. S. Lintuvuori, A. F. McVey, D. Marenduzzo, and W. C. Poon, *A growing bacterial colony in two dimensions as an active nematic*, *Nature Communications* **9**, 4190 (2018).
- [6] N. van den Berg, K. Thijssen, T. T. Nguyen, A. Sarlet, M. Cordero, A. G. Vázquez, N. Mitarai, A. Doostmohammadi, and L. Jauffred, *Emergent collective alignment gives competitive advantage to longer cells during range expansion*, *bioRxiv*, 2024 (2024).
- [7] G. Duclos, S. Garcia, H. G. Yevick, and P. Silberzan, *Perfect nematic order in confined monolayers of spindle-shaped cells*, *Soft Matter* **10**, 2346 (2014).
- [8] K. Copenhagen, R. Alert, N. S. Wingreen, and J. W. Shaevitz, *Topological defects promote layer formation in Myxococcus xanthus colonies*, *Nature Physics* **17**, 211 (2021).
- [9] G. Duclos, C. Erlenkämper, J.-F. Joanny, and P. Silberzan, *Topological defects in confined populations of spindle-shaped cells*, *Nature Physics* **13**, 58 (2017).
- [10] I. Ruider, K. Thijssen, D. R. Vannier, V. Paloschi, A. Sciortino, A. Doostmohammadi, and A. Bausch, *Topological excitations govern ordering kinetics in endothelial cell layers*, *bioRxiv*, 2024 (2024).
- [11] B. Senyuk, J. S. Evans, P. J. Ackerman, T. Lee, P. Manna, L. Vigderman, E. R. Zubarev, J. van de Lagemaat, and I. I. Smalyukh, *Shape-dependent oriented trapping and scaffolding of plasmonic nanoparticles by topological defects for self-assembly of colloidal dimers in liquid crystals*, *Nano Letters* **12**, 955 (2012).
- [12] T. Ohzono and J.-i. Fukuda, *Zigzag line defects and manipulation of colloids in a nematic liquid crystal in microwrinkle grooves*, *Nature Communications* **3**, 701 (2012).
- [13] J. M. Kosterlitz, *Topological defects and phase transitions*, *Nobel Physics Lecture* (2016).
- [14] M. J. Bowick, N. Fakhri, M. C. Marchetti, and S. Ramaswamy, *Symmetry, thermodynamics, and topology in active matter*, *Physical Review X* **12**, 010501 (2022).
- [15] A. Ardaševa and A. Doostmohammadi, *Topological defects in biological matter*, *Nature Reviews Physics* **4**, 354 (2022).
- [16] M. Kralj, M. Kralj, and S. Kralj, *Topological defects in nematic liquid crystals: Laboratory of fundamental physics*, *Physica Status Solidi (a)* **218**, 2000752 (2021).
- [17] T. B. Saw, A. Doostmohammadi, V. Nier, L. Kocgozlu, S. Thampi, Y. Toyama, P. Marcq, C. T. Lim, J. M. Yeomans, and B. Ladoux, *Topological defects in epithelia govern cell death and extrusion*, *Nature* **544**, 212 (2017).
- [18] K. Kawaguchi, R. Kageyama, and M. Sano, *Topological defects control collective dynamics in neural progenitor cell cultures*, *Nature* **545**, 327 (2017).
- [19] U. Tkalec and I. Muševič, *Topology of nematic liquid crystal colloids confined to two dimensions*, *Soft Matter* **9**, 8140 (2013).
- [20] L. C. Head, Y. A. G. Fosado, D. Marenduzzo, and T. N. Shendruk, *Entangled nematic disclinations using multi-particle collision dynamics*, *Soft Matter* **20**, 7157 (2024).
- [21] S. Čopar, U. Tkalec, I. Muševič, and S. Žumer, *Knot theory realizations in nematic colloids*, *Proceedings of the National Academy of Sciences* **112**, 1675 (2015).
- [22] K. Wamsler, L. C. Head, and T. N. Shendruk, *Lock-key microfluidics: simulating nematic colloid advection along wavy-walled channels*, *Soft Matter* **20**, 3954 (2024).
- [23] A. Modin, B. Ash, K. Ishimoto, R. L. Leheny, F. Serra, and H. Aharoni, *Tunable three-dimensional architecture of nematic disclination lines*, *Proceedings of the National*

- Academy of Sciences **120**, e2300833120 (2023).
- [24] S. Shankar, S. Ramaswamy, M. C. Marchetti, and M. J. Bowick, Defect unbinding in active nematics, *Physical Review Letters* **121**, 108002 (2018).
- [25] S. P. Thampi, R. Golestanian, and J. M. Yeomans, Velocity correlations in an active nematic, *Physical Review Letters* **111**, 118101 (2013).
- [26] A. Doostmohammadi, J. Ignés-Mullol, J. M. Yeomans, and F. Sagués, Active nematics, *Nature Communications* **9**, 3246 (2018).
- [27] L. Giomi, M. J. Bowick, P. Mishra, R. Sknepnek, and M. Cristina Marchetti, Defect dynamics in active nematics, *Philosophical Transactions of the Royal Society A: Mathematical, Physical and Engineering Sciences* **372**, 20130365 (2014).
- [28] S. Shankar and M. C. Marchetti, Hydrodynamics of active defects: From order to chaos to defect ordering, *Physical Review X* **9**, 041047 (2019).
- [29] R. Alert, J. Casademunt, and J.-F. Joanny, Active turbulence, *Annual Review of Condensed Matter Physics* **13**, 143 (2022).
- [30] P. W. Ellis, D. J. Pearce, Y.-W. Chang, G. Goldsztein, L. Giomi, and A. Fernandez-Nieves, Curvature-induced defect unbinding and dynamics in active nematic toroids, *Nature Physics* **14**, 85 (2018).
- [31] J. Hardoüin, C. Doré, J. Laurent, T. Lopez-Leon, J. Ignés-Mullol, and F. Sagués, Active boundary layers in confined active nematics, *Nature Communications* **13**, 6675 (2022).
- [32] P. Guillaumat, Ž. Kos, J. Hardoüin, J. Ignés-Mullol, M. Ravnik, and F. Sagués, Active nematic emulsions, *Science Advances* **4**, eaao1470 (2018).
- [33] G. Negro, L. C. Head, L. N. Carenza, T. N. Shendruk, D. Marenduzzo, G. Gonnella, and A. Tiribocchi, Topology controls flow patterns in active double emulsions, *Nature Communications* **16**, 1 (2025).
- [34] C. Valeriani, M. Li, J. Novosel, J. Arlt, and D. Marenduzzo, Colloids in a bacterial bath: simulations and experiments, *Soft Matter* **7**, 5228 (2011).
- [35] A. Lagarde, N. Dagès, T. Nemoto, V. Démery, D. Bartolo, and T. Gibaud, Colloidal transport in bacteria suspensions: from bacteria collision to anomalous and enhanced diffusion, *Soft Matter* **16**, 7503 (2020).
- [36] B. Loewe and T. N. Shendruk, Passive Janus particles are self-propelled in active nematics, *New Journal of Physics* **24**, 012001 (2022).
- [37] A. J. H. Houston and G. P. Alexander, Colloids in two-dimensional active nematics: conformal cogs and controllable spontaneous rotation, *New Journal of Physics* **25**, 123006 (2023).
- [38] L. Neville, J. Eggers, and T. B. Liverpool, Controlling wall-particle interactions with activity, *Soft Matter* **20**, 8395 (2024).
- [39] T. N. Shendruk and J. M. Yeomans, Multi-particle collision dynamics algorithm for nematic fluids, *Soft Matter* **11**, 5101 (2015).
- [40] Z. K. Valei, K. Wamsler, A. J. Parker, T. A. Obara, A. R. Klotz, and T. N. Shendruk, Dynamics of polymers in coarse-grained nematic solvents, *Soft Matter* **21**, 361 (2025).
- [41] E. J. Hemingway, P. Mishra, M. C. Marchetti, and S. M. Fielding, Correlation lengths in hydrodynamic models of active nematics, *Soft Matter* **12**, 7943 (2016).
- [42] L. Giomi, M. J. Bowick, P. Mishra, R. Sknepnek, and M. Cristina Marchetti, Defect dynamics in active nematics, *Philosophical Transactions of the Royal Society A* **372**, 20130365 (2014).
- [43] S. P. Thampi, R. Golestanian, and J. M. Yeomans, Instabilities and topological defects in active nematics, *Europhysics Letters* **105**, 18001 (2014).
- [44] L. C. Head, C. Doré, R. R. Keogh, L. Bonn, G. Negro, D. Marenduzzo, A. Doostmohammadi, K. Thijssen, T. López-León, and T. N. Shendruk, Spontaneous self-constraint in active nematic flows, *Nature Physics* (2024).
- [45] I. Musevic, M. Skarabot, U. Tkalec, M. Ravnik, and S. Zumer, Two-dimensional nematic colloidal crystals self-assembled by topological defects, *Science* **313**, 954 (2006).
- [46] M. Škarabot, M. Ravnik, S. Žumer, U. Tkalec, I. Poberaj, D. Babič, and I. Mušević, Hierarchical self-assembly of nematic colloidal superstructures, *Physical Review E* **77**, 061706 (2008).
- [47] S. Ray, J. Zhang, and Z. Dogic, Rectified rotational dynamics of mobile inclusions in two-dimensional active nematics, *Physical Review Letters* **130**, 238301 (2023).
- [48] F. Guzmán-Lastra, H. Löwen, and A. J. Mathijssen, Active carpets drive non-equilibrium diffusion and enhanced molecular fluxes, *Nature Communications* **12**, 1906 (2021).